Heliyon 10 (2024) e28876

Contents lists available at ScienceDirect

Heliyon

journal homepage: www.cell.com/heliyon

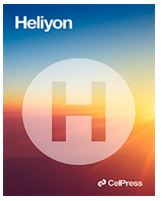

Research article

Translatome and transcriptome profiling of neonatal mice hippocampus exposed to sevoflurane anesthesia

Menghan Wang, Limin Zhang, Hecheng Yang, Hong Lu *

Department of Neurology, The First Affiliated Hospital of Zhengzhou University, Zhengzhou 450052, Henan, China

ARTICLE INFO

Keywords:
Sevoflurane anesthesia
RNA sequencing
Mice hippocampus
Cognitive impairment
Translatome

ABSTRACT

Exposure to anesthesia in early life may cause severe damage to the brain and lead to cognitive impairment. The underlying mechanisms, which have only been investigated in a limited scale, remains largely elusive. We performed translatome and transcriptome sequencing together for the first time in hippocampus of neonatal mice that were exposed to sevoflurane. We treated a group of neonatal mice with 2.5 % sevoflurane for 2 h on day 6, 7, 8, 9 and treated another group on day 6, 7. We performed behavioral study after day 30 for both groups and the control to evaluate the cognitive impairment. On day 36, we collected translatome and transcriptome from the hippocampus in the two groups, compared the gene expression levels between the groups and the control, and validated the results with RT-qPCR. We identified 1750 differentially expressed genes (DEGs) from translatome comparison and 1109 DEGs from transcriptome comparison. As expected, translatome-based DEGs significantly overlapped with transcriptome-based DEGs, and functional enrichment analysis generated similar enriched cognition-related GO terms and KEGG pathways. However, for many genes like Hspa5, their alterations in translatome differed remarkably from those in transcriptome, and Western blot results were largely concordant with the former, suggesting that translational regulation plays a significant role in cellular response to sevoflurane. Our study revealed global alterations in translatome and transcriptome of mice hippocampus after neonatal exposure to sevoflurane anesthesia and highlighted the importance of translatome analysis in understanding the mechanisms responsible for anesthesia-induced cognitive impairment.

1. Introduction

Ample clinical investigations have shown that widespread use of anesthetic reagent in early life, especially in early childhood, posts threat to proper brain development and may cause severe cognitive impairment [1,2]. In a recent study consisting of 20,922 children from US [3], nearly 15 % have went through surgical operations with general anesthesia before the age of 3. Among them, approximately 25 % have underwent multiple anesthesia exposures and are at higher risk of developing behavioral changes and long-term disorders in cognitive function and learning ability [4–6].

Recent clinical studies have shown that, although anesthesia of about 1 h for children under the age of 3 would not have a great impact on brain development [7,8], repeated or prolonged anesthesia exposures are reported to cause problems in behaviors and executive functions [9]. A more recent prospective study has further shown that children who had multiple exposures to anesthesia

* Corresponding author.
E-mail address: zzu_luhong@163.com (H. Lu).

https://doi.org/10.1016/j.heliyon.2024.e28876
Received 21 March 2023; Received in revised form 21 March 2024; Accepted 26 March 2024
Available online 12 April 2024

would have problems in processing speed and fine motor abilities [10]. Similarly, animal studies have also shown that neonatal exposures to anesthesia in the young mice can induce neuroinflammation, synaptic dysfunction and Tau phosphorylation [11–14]. These studies have promoted the proper use and deeper understanding of anesthesia, but the underlying molecular mechanisms remain to be further explored.

Sevoflurane is the most commonly used inhalational anesthetic reagent in children, with good properties like rapid onset and offset, respiratory tolerance and hemodynamic stability [15]. Multiple neonatal sevoflurane exposures also lead to visual recognition memory loss, learning impairment and abnormal behaviors in model organisms such as mouse and rhesus macaque [16–18], highlighting the need for more studies on sevoflurane using appropriate anesthesia protocols. On the other hand, the hippocampus, a key region of the brain, play a vital role in cognition, memory and navigation [19]. Recent studies using animal models have demonstrated that knockout of certain genes in hippocampus leads to the loss of multiple cognitive functions, thus making hippocampus a good candidate for studying anesthesia-induced cognitive impairment [20,21].

To reduce impairment caused by anesthesia and explore potential therapeutic interventions, it is of great importance to understand the dysregulation of gene expression responsible for the impairment on a genome-wide scale. Gene expression is regulated at several levels, among which translational regulation controls nearly half of the variation in protein concentration [22,23]. Since the polysome-associated RNA (i.e., translatome) reflects the effective readout of the genome in a given cell at a given time point, interrogating translatome brings us a deeper understanding of gene expression regulation and could also explain the differences between transcriptome and proteome analysis [24–26]. Translatome sequencing based on sucrose-gradient separation of polysome-associated RNAs is the most commonly used technique for investigating translatome [27]. This technique (also called polysome profiling) has been widely used for specific mRNA analysis as well as for genome-wide analysis [27–30].

In this study, we used neonatal mice as the model to investigate the dysregulation of gene expression after multiple exposures to sevoflurane. We used behavioral studies to assess the cognitive impairment in two groups of mice with different levels of sevoflurane exposures and compared the results with the normal group. We then collected polysome-associated RNA and total RNA (i.e., transcriptome) from the hippocampus of the sevoflurane-treated groups and the normal group and performed detailed comparison among the groups with high-throughput sequencing data. We used RT-qPCR to further validate the sequencing results and used Western blot to confirm the protein abundance alteration when divergence between translatome and transcriptome arose. This study demonstrated the importance of translatome sequencing in understanding the mechanisms responsible for anesthesia-induced cognitive impairment, underscoring the necessity of translatome analysis in future studies.

2. Materials and methods

2.1. Mice anesthesia using sevoflurane

In accordance with the Guide for the Care and Use of Laboratory Animals from the National Institutes of Health, we conducted animal experiments that were approved by the ethics committee of the First Affiliated Hospital of Zhengzhou University under the experimental protocol LLS-2021-034NZ. Thirty C57BL/J6 mice were acquired from Shanghai SLAC Laboratory Animal in Shanghai, China, and were randomly assigned to three groups of ten mice each using the function “sample” in the R environment (http://www.r-project.org/). The mice were housed in a controlled environment with standard rodent food and water provided ad libitum. The mice were anesthetized with sevoflurane according to a previously published protocol [12]. Group A received 2.5 % sevoflurane with 60 % O2 at a flow rate of 2 L/min for 3 min and 1 L/min for 2 h on postnatal days 6, 7, 8, and 9 (i.e., four exposures), while Group B received the same anesthetic regimen on postnatal days 6 and 7 (i.e., two exposures). The control group received 60 % O_2 at the same flow rate in the same anesthetizing chamber. The anesthetizing chamber was maintained at a warm temperature to maintain the mice’s rectal temperature at 37 $\pm$ 0.5 °C.

2.2. Arterial blood gas analysis

Blood samples were obtained from the abdominal aorta of five mice from each group at two different time points: 5 min and 115 min during anesthesia on day 9 of the experiment. The blood samples were immediately analyzed using a blood gas analyzer (ABL80 FLEX, Radiometer, Carlsbad, USA). The values of several parameters, including partial pressures of O2 and CO2, hematocrit, pH, and levels of Ca+, Na+, K+, and Cl-, were recorded.

2.3. Morris water maze experiments

A Morris water maze (MWM) experiment was conducted to evaluate spatial learning and memory function, following a previously described protocol [31]. The MWM device was filled with opaque water, and a platform (diameter, 10 cm) was submerged below the water’s surface. The temperature of the water was maintained at 22 °C, and the surrounding environment was kept very quiet during the experiments. The mice were trained for 5 consecutive days (from day 30 to day 34) with four trials each day, and escape latency, the time taken by the mice to reach the platform, was recorded to evaluate spatial learning. On day 35, testing experiments were conducted, and mean distance from the original platform area, platform-crossing times, and time spent in the fourth quadrant (the platform quadrant) were recorded to assess memory function. The mice were dried using a heat lamp to maintain their body temperature before being returned to their home cages.

2.4. RNA extraction and library preparation

On day 36, the mice were sacrificed through cervical dislocation. Following this, the scalp was cut open, and the skull was dissected through a sagittal suture. The cerebral cortex was found and removed, and the hippocampus was located under the cerebral cortex and isolated from the surrounding brain tissues. The isolation of the polysome fraction was conducted using a method from a previous study, with minor modifications [32]. The hippocampus tissues were lysed (in replicates) in a Polytron with 400 μL lysis buffer containing 100 μg/mL cycloheximide. The lysates were incubated on ice for 10 min and then centrifuged at 10000×*g* for 10 min at 4 °C. The supernatants were collected and loaded into 10–50 % sucrose gradients. The gradients were then placed in a Beckman SW41Ti rotor and centrifuged at 39,000 rpm at 4 °C for 2.5 h to collect the polysome fractions. Polysome-associated RNA was extracted with TRIZOL according to the manufacturer's protocol (Invitrogen, Waltham, USA), while total RNA was extracted directly from the hippocampus tissues (in replicates) using the same TRIZOL protocol.

The extracted RNA was subjected to DNase treatment for removing genomic DNA contamination. NEBNext PolyA mRNA Magnetic Isolation Module (New England Biolabs, Ipswich, USA) was employed for isolation of mRNA, which was subsequently utilized for sequencing library preparation with NEB Next Ultra Directional RNA Library Prep Kit for Illumina (New England Biolabs, Ipswich, USA). The libraries were quantified using Qubit 4.0 (Thermo Fisher Scientific, Waltham, USA) and the distribution of fragment sizes was evaluated using Agilent Bioanalyzer 2100 (Agilent, Santa Clara, USA). Illumina sequencing was performed on the libraries with paired-end 2x150 as the sequencing mode.

2.5. Sequencing data analysis

High-quality clean reads were obtained by removing sequencing adapters and low-quality reads using Cutadapt v1.18 (with default parameters except –max-n 0) and Trimmomatic v0.35 (with default parameters except SLIDINGWINDOW:4:15 LEADING:10 TRAILING:10) [33,34]. The clean reads were then checked for high quality using FastQC (with default parameters) to ensure accuracy (https://www.bioinformatics.babraham.ac.uk/projects/fastqc/). The mouse genome (assembly GRCm38) was used as a reference for mapping the clean reads with HISAT2 v2.1.0 (with default parameters except –rna-strandness RF –dta) [35].

The measurement of gene expression levels was performed by utilizing FPKM (fragments per kilobase of exon per million fragments mapped), which was conducted using StringTie v1.3.4 (with default parameters except -e –rf) [36]. In order to identify differentially expressed genes (DEGs), the R package, edgeR, was employed [37]. Genes with p-values <0.05 and $|\log 2(\text{Fold Change})| > 1$ were considered differentially expressed and utilized for downstream analysis.

The Ensembl genome browser 96 database (http://www.ensembl.org/index.html) was used to retrieve mouse gene annotation files. To annotate genes with gene ontology (GO) terms and Kyoto Encyclopedia of Genes and Genomes (KEGG) pathways, the R package of ClusterProfiler was employed [38–40]. The functional enrichment analysis based on GO and KEGG was also conducted using ClusterProfiler.

2.6. Western blot analysis

The homogenization of hippocampus tissues from mice (in triplicates from each group, different from those used in RNA-seq experiments) was carried out using a Dounce Tissue Homogenizer (BioVision, Milpitas, USA) with RIPA lysis buffer as per the manufacturer's protocol. The protein concentrations were quantified using Bradford protein assay reagent (Bio-Rad, Hercules, USA). The samples were resolved by 8–12 % SDS-PAGE and transferred to nitrocellulose membranes (Millipore, Bedford, USA). The primary antibodies (PSD-95: 1:2000, #3450, Cell Signaling Technology, Beverly, USA; Galr2: 1:2000, ab96702, Abcam, Cambridge, USA; Lcn2: 1:2000, ab216462, Abcam, Cambridge, USA; Hspa5: 1:2000, ab21685, Abcam, Cambridge, USA) were used to immunoblot aliquots of proteins at 4 °C overnight. The membranes were then incubated with secondary antibodies at room temperature for 1 h. Following immunoblotting, the membranes were developed using ECL (Enhanced Chemiluminescence) Plus reagents (Beyotime Biotechnology, Shanghai, China). Normalization of protein expression levels was performed relative to β-actin (AA128, Beyotime Biotechnology, Shanghai, China). The analysis of Western blot images was conducted using the Image J software (Bio-Rad, Hercules, USA).

2.7. Real-time quantitative PCR

Polysome-associated RNA and total RNA were extracted using TRIZOL reagent (Life Technologies, Carlsbad, USA) and cDNA was synthesized with SuperScript III (Life Technologies, Carlsbad, USA). Real-time quantitative PCR (RT-qPCR) was conducted in triplicates (i.e., three mice per group that were different from those used in RNA-seq experiments) with a SYBR Green MasterMix (DBI Bioscience, Shanghai, China) following the manufacturer's instructions. The Applied Biosystems StepOnePlus system (Applied Biosystems, Foster City, USA) was employed to generate a threshold cycle (Ct), as per the manufacturer's protocol. ΔΔCt method was used to compute gene expression values, using Actb as the reference. The primer sequences were synthesized by Sangon Biotech (Shanghai, China) and obtained from PrimerBank [41].

2.8. Statistical analysis

All the statistical analyses were performed with the R language. The statistical difference of escape latency, average distance, platform-crossing times, and time spent in the 4th quadrant in the MWM experiment was assessed using Student's t-test. Additionally,

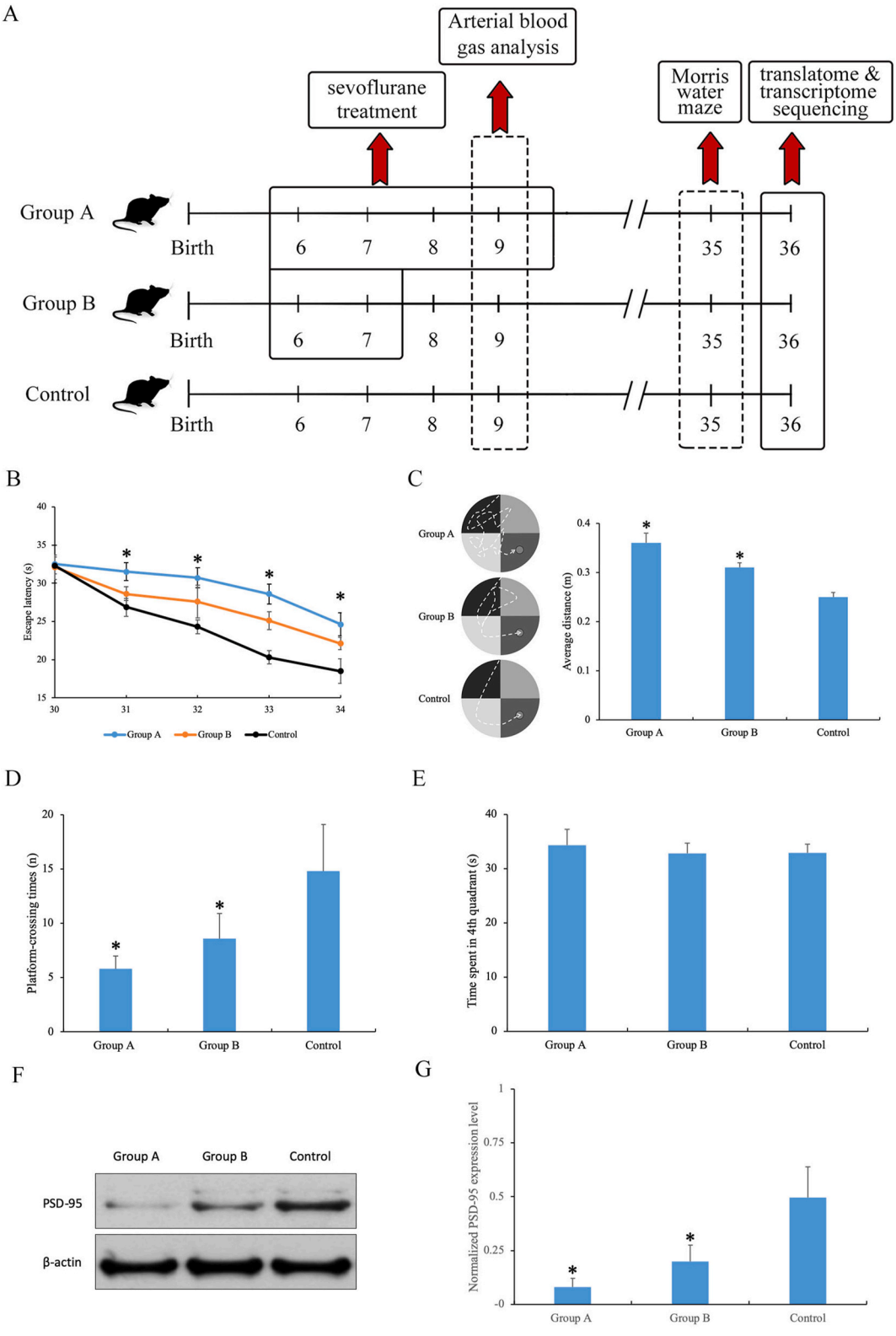

(caption on next page)

Fig. 1. The design of the study and the evaluation of cognitive impairment. (A) The study design for Group A and B with time points of sevoflurane treatment, arterial blood gas analysis, MWM experiment and RNA-seq analysis. (B) MMW (training experiment on day 30–34) comparing the scape latency between groups. (C, D, E) MWM (testing experiment on day 35) comparing the average distance from original platform area, platform-crossing times and the time spent in the fourth quadrant between Group A, B and the control. (F, G) Western blot analysis of the PSD-95 levels in the hippocampus of mice collected on day 36. Quantification of Western blot is shown on the right side. "*" indicates statistical difference in all panels.

Student's t-test was used to calculate the p-values for fold change difference in RT-qPCR validation. Fisher's exact test was used to calculate the p-values in functional enrichment analysis.

3. Results

3.1. Study design and evaluation of sevoflurane-induced cognitive impairment

The design of this study was briefly illustrated in Fig. 1A. In Group A and B, the neonatal mice were treated with sevoflurane as mentioned above, after which MWM experiments were conducted. The hippocampus tissues were harvested on day 36, from which total RNA and polysome-associated RNA were collected for RNA sequencing.

We first performed arterial blood gas analysis to exclude the possibility that the MWM experiment results were owing to poor oxygenation. On day 9, we took arterial blood from the mice treated with sevoflurane and analysis with the blood gas analyzer showed that values of partial pressures of O_2 and CO_2, hematocrit, pH, Ca^+, Na^+, K^+, and Cl^- were all within the normal ranges with no significant difference between the values measured at 5 min and 115 min during anesthesia on day 9 (all p-values >0.05, Wilcoxon rank sum test; table S7).

We then evaluated the cognitive impairment of the three groups with MWM experiments. In the training experiments from day 30–34, mice from Group A had the longest escape latency (34.3 ± 2.9; Fig. 1B), which was followed by Group B (22.8 ± 1.9), and the control group had the shortest escape latency (12.9 ± 1.6). In the testing experiments conducted on day 35, mice from Group A had the longest average distance from the platform (0.36 ± 0.02), followed by mice from Group B (0.31 ± 0.01), and mice from the control group had the shortest average distance (0.25 ± 0.01; Fig. 1C). For platform-crossing times, the control group had the best performance, followed by Group B and then by Group A (Fig. 1D). The time spent in the fourth quadrant did not vary significantly among the three groups (p-value >0.05, Student's t-test; Fig. 1E). These results showed that cognitive impairment was noticeable in Group B and much more severe in Group A with more sevoflurane exposures.

We further compared the protein abundance of postsynaptic density protein-95 (PSD-95) in the hippocampus among Group A, B and the control. PSD-95 is a postsynaptic marker and its abundance would be decreased in mice hippocampus after neonatal exposures to sevoflurane [42]. Here we observed moderate and remarkable abundance reduction of PSD-95 respectively in the hippocampus of Group B and A as compared with the control (Fig. 1F and G), which was consistent with the previous studies [12] and our MWM results.

3.2. Differentially expressed genes identified by translatome sequencing

Based on the extracted polysome-associated RNA, we prepared two sequencing libraries (in replicates) for each group and obtained approximately 336 million reads (150 bp in length) in total. After data quality control and sequence alignment, we quantified gene expression levels with FPKM and identified a total of 24,646 expressed genes among the three groups (table S1). With these expressed genes, we carried out principal component analysis (PCA) and correlation analysis among all replicates. As expected, the replicates from the same group were located much closer than those from different groups in PCA (Fig. 2A), and that Pearson correlation coefficients were much higher in the same group than between groups (Fig. 2B). We then performed differential expression analysis and identified 1135 DEGs between Group A and B and 961 DEGs between Group B and the control (Fig. 2C). 685 of the 1135 DEGs and 721 of the 961 DEGs were up-regulated and the rest were down-regulated, whose expression patterns distinguished the sevoflurane-treated groups from the control (Fig. 2D).

Based on the DEGs, we first performed enrichment analysis with GO terms in the category of biological process. We identified "hindbrain development", "cerebellum morphogenesis" and "G2 DNA damage checkpoint" as the top 3 enriched GO terms for the 1135 DEGs and "NADP metabolic process", "hindbrain development" and "cerebellum morphogenesis" for the 961 DEGs (Fig. 3A). As expected, GO terms related to cognitive function were in the list of enrichment, such as synapse assembly and nervous system development. GO terms in the categories of molecular functions and cellular component were also used for enrichment analysis and all GO-based results were listed in table S2. We then performed KEGG-based enrichment analysis and revealed "GABAergic synapse", "Neuroactive ligand-receptor interaction" and "Glutamatergic synapse" as the top 3 enriched pathways for the 1135 DEGs and "Neuroactive ligand-receptor interaction", "Vitamin digestion and absorption" and "Glutamatergic synapse" for the 961 DEGs (Fig. 3B). Similar to GO-based results, we also observed cognitive function-related KEGG pathways in the top 20 list, such as "glutamatergic synapse", "Cholinergic synapse" and "Alzheimer disease". All KEGG-based results were listed in table S3.

We used the R language to randomly selected 5 genes (Pdzd4, Efr3b, Ldb1, Pcnt, Scn5a) from the top 50 genes that were up-regulated after sevoflurane exposure and used RT-qPCR to validate their differential expression among the three groups. RT-qPCR validated the significant up-regulation for 4 genes (Fig. 3C). Similar, we randomly selected 5 genes (Tspan5, Pram 1, Nmb, Spcs1 and Rnf227) down-regulated after sevoflurane exposure and validated the significant down-regulation of all 5 genes using RT-qPCR

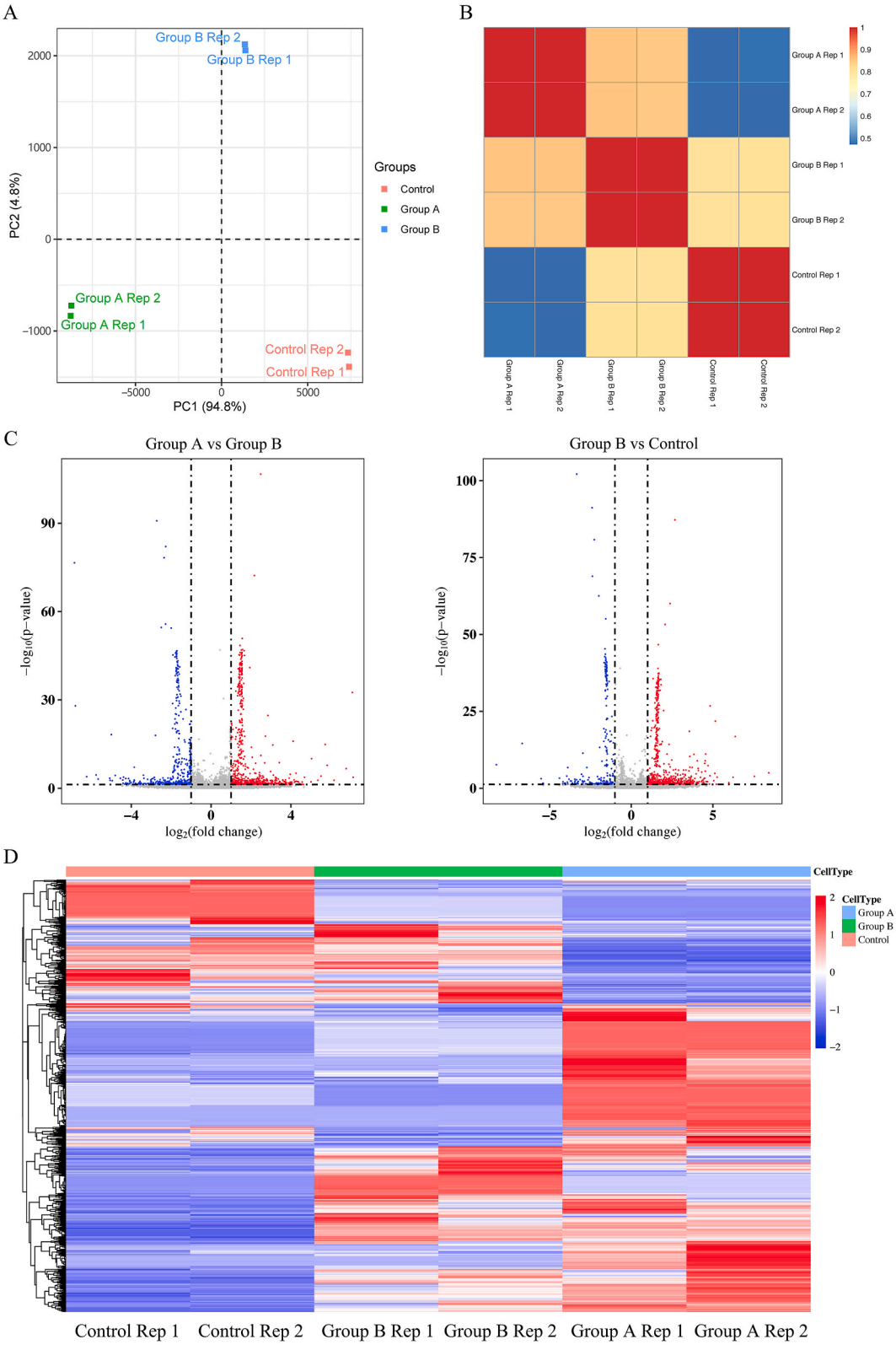

(caption on next page)

Fig. 2. Translatome-based gene expression analysis. (A) PCA of mice hippocampus translatome from Group A, B and the control. The 94.8 % and 4.8 % are the percentage of variance explained by PC1 and PC2. (B) Pairwise Pearson correlation among all samples (translatome) from the three groups. The colors in the top-right color bar represent the Pearson correlation coefficient (r). (C) Volcano plot of the DEGs between Group A and B, Group B and the control. Red points represent up-regulated DEGs; blue ones represent down-regulated DEGs; the rest (not differentially expressed genes) are marked with gray. (D) Heatmap of the DEGs among all three groups. The color represents the standardized values of gene expression, which is shown in the top-right color bar. (For interpretation of the references to color in this figure legend, the reader is referred to the Web version of this article.)

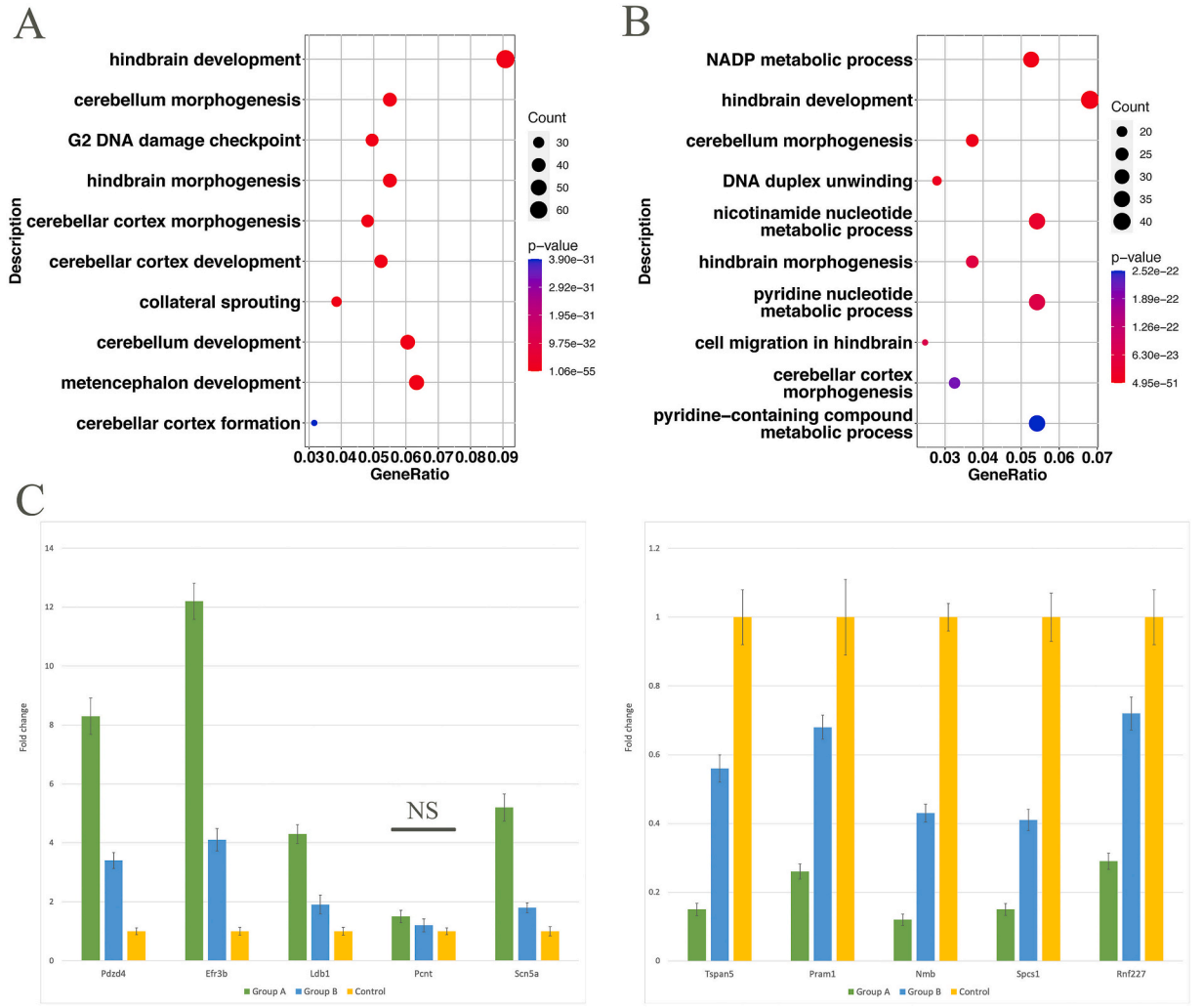

Fig. 3. Functional enrichment analysis and RT-qPCR validation. (A) Dotplot for the results of GO-based functional enrichment analysis. "GeneRatio" equals the number of DEGs divided by the total number of genes in the pathway. The dot size stands for the number of DEGs in the pathway and the dot color stands for the p-value. (B) Dotplot for the results of KEGG-based functional enrichment analysis. The definitions of "GeneRatio", dot size and color are the same as in (A). (C) RT-qPCR validation for 10 DEGs identified by translatome sequencing. The left and right panels show the RT-qPCR results of genes up-regulated and down-regulated in translatome after sevoflurane exposure, respectively. Fold change has been normalized with respect to the control. "NS" indicates no statistical difference, and those without "NS" label have statistical difference. (For interpretation of the references to color in this figure legend, the reader is referred to the Web version of this article.)

(Fig. 3C; the primer sequences were listed in table S4).

3.3. Differentially expressed genes identified by transcriptome sequencing

Based on the extracted total RNA, we prepared two sequencing libraries (in replicates) for each group and obtained approximately 303 million reads (150 bp in length) in total. With the same methods described above, we carried out PCA and correlation analysis to support the high quality of the sequencing libraries (figs. S1 and S2) and identified a total of 26,937 expressed genes among the three

groups. Differential expression analysis revealed 862 DEGs between Group A and B and 452 DEGs between Group B and the control, among which 579 and 274 were up-regulated, respectively (Fig. 4A; fig. S3). Not surprisingly, the top 100 DEGs significantly overlapped with their counterparts from translatome (p-values <0.001, Fisher's exact test).

Based on the DEGs, we performed GO and KEGG-based enrichment analysis as described above. We identified "hindbrain development", "cell differentiation in hindbrain" and "cerebellar cortex formation" as the top 3 enriched GO biological process for the 862 DEGs and "bone trabecula morphogenesis", "bone trabecula formation" and "hindbrain development" for the 452 DEGs (table S6). We identified "Glutamatergic synapse", "Pathways of neurodegeneration - multiple diseases" and "Cholinergic synapse" as the top 3 enriched KEGG pathways for the 862 DEGs and "Glutamatergic synapse", "Alzheimer disease" and "Pathways of neurodegeneration - multiple diseases" for the 452 DEGs (table S6). The top 20 enriched GO terms and KEGG pathways significantly overlapped with those from translatome (p-values <0.05, Fisher's exact test), which was consistent with the significant overlap between DEGs. We also used

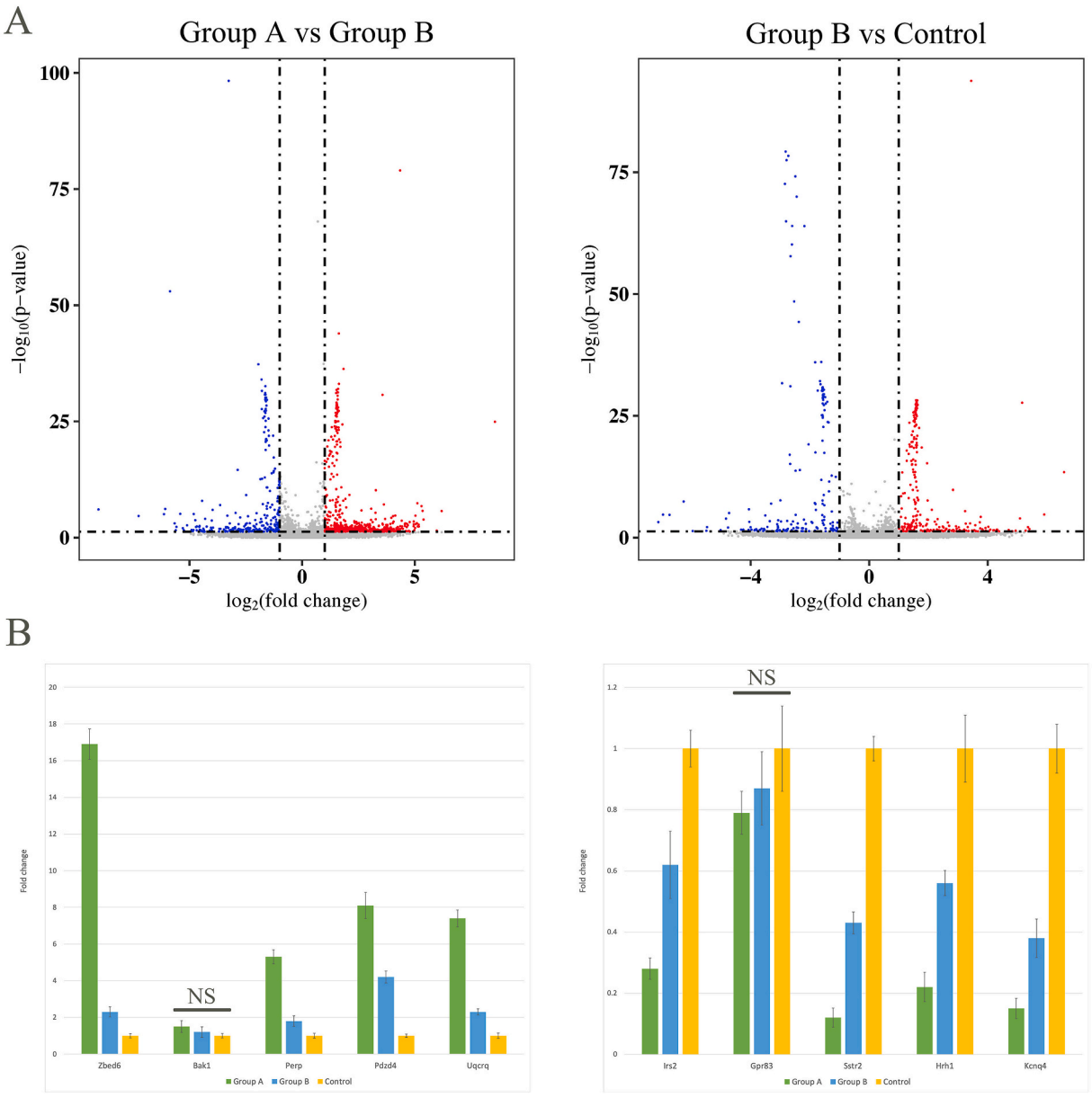

Fig. 4. Differential expression analysis and RT-qPCR validation. (A) Volcano plot of the transcriptome-based DEGs between Group A and B, Group B and the control. Red points stand for up-regulated DEGs and blue ones stand for down-regulated DEGs. (B) RT-qPCR validation for 10 DEGs identified by transcriptome sequencing. The left and right panels show the RT-qPCR results of genes up-regulated and down-regulated in transcriptome after sevoflurane exposure, respectively. Fold change has been normalized with respect to the control. "NS" indicates no statistical difference. (For interpretation of the references to color in this figure legend, the reader is referred to the Web version of this article.)

RT-qPCR to validate the DEGs with the method described above: the 5 genes up-regulated after sevoflurane exposure were Zbed6, Bak 1, Perp, Pdzd4 and Uqcrq, and the 5 genes down-regulated were Irs 2, Gpr83, Sstr2, Hrh1 and Kcnq4. RT-qPCR validated the significant up-regulation and down-regulation of 8 genes (Fig. 4B; the primer sequences were listed in table S4).

3.4. Divergence between translatome and transcriptome

Based on the expression levels of each gene in the three groups, we calculated the Pearson correlation coefficient (r) of the levels between translatome and transcriptome. Low positive correlations ($0< r < 0.3$) or even negative correlations ($r < 0$) was observed for a noticeable number of genes, indicating the divergence between translatome and transcriptome (Fig. 5A). Here, we selected the top 500 DEGs from translatome and transcriptome, which were often studied in RNA-seq analysis, and investigated the expression patterns of these genes. Among these top DEGs, we observed two typical patterns (Fig. 5B) [1]: the fold changes were much larger in translatome than in transcriptome (e.g., Galr2), and [2] the fold changes were much smaller in translatome (e.g., Lcn2). As shown in Fig. 5A, a small

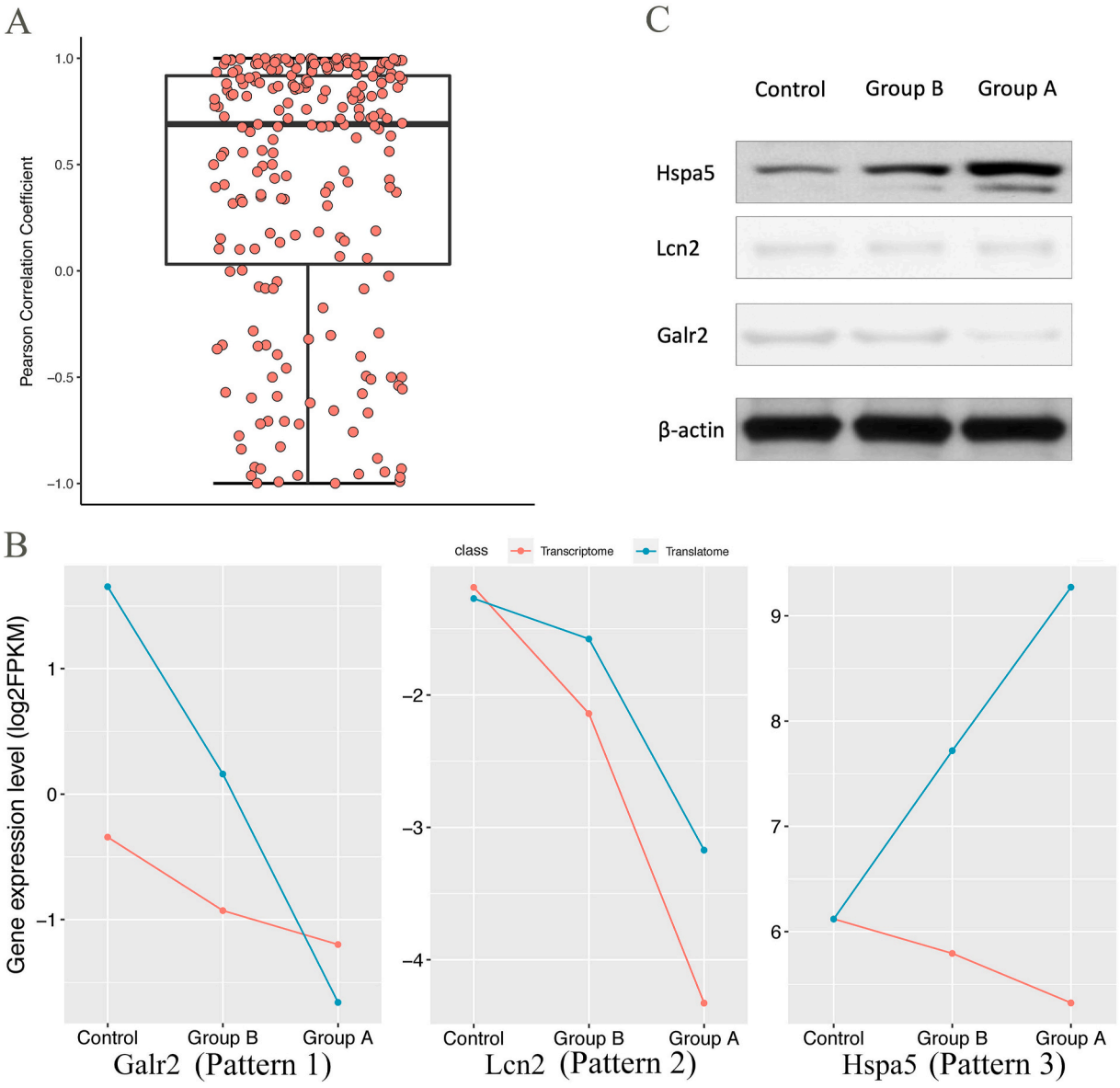

Fig. 5. Correlation analysis and Western blot validation. (A) The correlation of gene expression between translatome and transcriptome. Each point represents a Pearson correlation coefficient calculated with the expression levels of a gene in Group A, B and the control. Only 1 % of data were randomly picked using R for better visualization. (B) Three examples with typical patterns of fold changes. Galr2 and Lcn2 had low positive correlation of expression levels between translatome and transcriptome, while Hspa5 had a high negative correlation. Gene names are shown below the three plots. (C) Western blot analysis of the three genes (Galr2, Lcn2 and Hspa5).

but non-negligible proportion of genes had moderate or high negative correlation, with Hspa5 as a typical example (Pattern 3 in Fig. 5B). We further perform Western blot analysis for the three typical genes in Fig. 5B and found that Western blot results were more concordant with the fold changes observed in translatome for all three genes (Fig. 5C; fig. S4). These results showed that differential expression analysis only based on transcriptome sequencing could lead to unreliable inference about the molecular mechanisms responsible for cognitive impairment.

4. Discussion

In this study, we investigated the genome-wide responses to sevoflurane exposures of neonatal mice based on translatome and transcriptome sequencing of the hippocampus. We compared the DEGs and enriched pathways between translatome and transcriptome and analyzed their similarity and divergence with RT-qPCR and Western blot as validation methods. This work has made at least three important contributions as follows to the understanding of molecular mechanisms involved in cognitive impairment induced by sevoflurane. First, this study has identified more than a thousand DEGs in both translatome and transcriptome and confirmed that they are highly consistent with each other; second, this study has revealed, for many genes, the divergence of their abundance between translatome and transcriptome, which demonstrates the importance of translatome sequencing in studies on anesthesia-induced cognitive impairment; third, this study accumulated 12 sets of RNA-seq data that could be analyzed with similar data from different times of sevoflurane exposure or with other types of omics data to better decipher the complicated regulatory mechanisms in future.

It is worth mentioning that genes in pattern 1 (Fig. 5B) were more inclined to be involved in pathways related to cognitive functions, such as synapse assembly and Alzheimer's disease (both p-values <0.05, Fisher's exact test). Further examination showed that several DEGs involved in cognitive functions had very large expression alterations (up to five times) in translatome than in transcriptome, suggesting that these genes had a much stronger response to sevoflurane in translational regulation. These genes at least include Grm2, Kcnj2, Gsk3b and BACE1. Further studies on these genes may help to uncover potential therapeutic targets for anesthesia-related diseases.

Exposures to sevoflurane in early life were shown to cause apoptosis in the hippocampus and cerebral cortex [43,44]. In this study, although we also identified significantly enriched GO terms involved in the cellular response to apoptotic process in both translatome and transcriptome analysis, the p-values of enrichment were generally larger (less significant) in translatome than in transcriptome. For example, the GO term GO:2,001,233 (regulation of apoptotic signaling pathway) had enrichment p-values less than 0.01 in transcriptome, but its p-value was not significant in translatome (p-value >0.05, Fisher's exact test). For another GO term GO:0097, 191 (extrinsic apoptotic signaling pathway), its enrichment p-value in transcriptome was much more significant (>1000 times smaller) than its counterpart in translatome. These results indicate that, although sevoflurane exposures may induce cellular response in apoptotic process, the response may not be as strong as previously expected.

Previous studies showed that children before the age of 3 who received three or more exposures to sevoflurane had a higher risk of developing cognitive impairment before the age of 15, while only one exposure would not significantly increase the risk [5, 7, 9]. In this study, transcriptome analysis in hippocampus showed that two exposures (Group B) to sevoflurane in neonatal mice led to differential expression of <100 genes involved in cognitive impairment and brain development; but more importantly, there existed much more DEGs (>2 times) in hippocampus translatome of two exposures (Group B) to sevoflurane, which had much smaller enrichment p-values in cognition-related pathways. These results indicate that, for neonatal mice, only two exposures to sevoflurane could already cause noticeable alterations in gene expression (especially in translation) and problems in behaviors, which could be an important information for the decision making of physicians.

RNA sequencing has been widely used for gene expression profiling in the studies of cognitive impairment. For example, Kaneshwaran et al., 2019 used RNA-seq to investigate the association between sleep fragmentation with cognitive impairment [45]; Brito et al., 2020 used RNA-seq data to identify a set of gene interactions that could be involved in cognitive and neurodegeneration processes [46]. In recent years, sequencing of the translating RNA has further promoted the understanding of cognitive impairment. For example, Kaczmarczyk et al., 2022 showed that early translatome responses to neurodegeneration emerge prior to conventional markers of disease [47]. Here we used translatome sequencing for the first time to investigate the impact of multiple exposure to sevoflurane anesthesia in neonatal mice, which further demonstrated the importance of RNA sequencing in understanding the mechanisms responsible for cognitive impairment in future studies.

5. Conclusion

This study has revealed global alterations in translatome and transcriptome of mice hippocampus after neonatal exposure to sevoflurane anesthesia; moreover, it has highlighted the importance of translatome analysis in understanding the underlying mechanisms responsible for anesthesia-induced cognitive impairment.

Ethics approval and consent to participate

This study was approved by the ethics committee of the First Affiliated Hospital of Zhengzhou University approved the experimental protocol (LLS-2021-034NZ). All participants signed informed consent prior to using the tissues for scientific research.

Consent for publication

All authors have consented to the publication of this manuscript.

Funding

None.

Data availability

We have submitted all translatome and transcriptome sequencing data generated in this study to the ArrayExpress database (http://www.ebi.ac.uk/arrayexpress) and the accession number is E-MTAB-10202.

CRediT authorship contribution statement

Menghan Wang: Methodology, Data curation. **Limin Zhang:** Resources, Formal analysis. **Hecheng Yang:** Methodology, Data curation. **Hong Lu:** Writing – review & editing, Conceptualization, Writing – original draft.

Declaration of competing interest

The authors declare that they have no known competing financial interests or personal relationships that could have appeared to influence the work reported in this paper.

Acknowledgements

Not applicable.

Abbreviations

DEG	differentially expressed gene
MWM	Morris water maze
GO	Gene Ontology
KEGG	Kyoto Encyclopedia of Genes and Genomes
RT-qPCR	real-time quantitative PCR
PCA	principal component analysis

Appendix A. Supplementary data

Supplementary data to this article can be found online at https://doi.org/10.1016/j.heliyon.2024.e28876.

References

[1] L. Sun, Early childhood general anaesthesia exposure and neurocognitive development, Br. J. Anaesth. (2010) i61–i68.
[2] L. Vutskits, Z. Xie, Lasting impact of general anaesthesia on the brain: mechanisms and relevance, Nat. Rev. Neurosci. 17 (11) (2016) 705–717.
[3] Y. Shi, D. Hu, E. Rodgers, S. Katusic, S. Gleich, A. Hanson, et al., Epidemiology of general anesthesia prior to age 3 in a population-based birth cohort, Paediatr. Anaesth. 28 (6) (2018) 513–519.
[4] A. Vinson, C. Houck, Neurotoxicity of anesthesia in children: Prevention and treatment, Curr. Treat. Options Neurol. 20 (12) (2018) 51.
[5] R. Wilder, R. Flick, J. Sprung, S. Katusic, W. Barbaresi, C. Mickelson, et al., Early exposure to anesthesia and learning disabilities in a population-based birth cohort, Anesthesiology 110 (4) (2009) 796–804.
[6] P. Glatz, R. Sandin, N. Pedersen, A. Bonamy, L. Eriksson, F. Granath, Association of anesthesia and Surgery during childhood with long-term Academic performance, JAMA Pediatr. 171 (1) (2017) e163470.
[7] L. Sun, G. Li, T. Miller, C. Salorio, M. Byrne, D. Bellinger, et al., Association between a single general anesthesia exposure before age 36 Months and neurocognitive outcomes in later childhood, JAMA 315 (21) (2016) 2312–2320.
[8] M. McCann, J. de Graaff, L. Dorris, N. Disma, D. Withington, G. Bell, et al., Neurodevelopmental outcome at 5 years of age after general anaesthesia or awake-regional anaesthesia in infancy (GAS): an international, multicentre, randomised, controlled equivalence trial, Lancet (London, England) 393 (10172) (2019) 664–677.
[9] D. Hu, R. Flick, M. Zaccariello, R. Colligan, S. Katusic, D. Schroeder, et al., Association between exposure of young children to procedures requiring general anesthesia and learning and behavioral outcomes in a population-based birth cohort, Anesthesiology 127 (2) (2017) 227–240.
[10] D. Warner, M. Zaccariello, S. Katusic, D. Schroeder, A. Hanson, P. Schulte, et al., Neuropsychological and behavioral outcomes after exposure of young children to procedures requiring general anesthesia: the mayo anesthesia safety in kids (MASK) study, Anesthesiology 129 (1) (2018) 89–105.
[11] X. Shen, Y. Dong, Z. Xu, H. Wang, C. Miao, S. Soriano, et al., Selective anesthesia-induced neuroinflammation in developing mouse brain and cognitive impairment, Anesthesiology 118 (3) (2013) 502–515.

[12] H. Lu, N. Liufu, Y. Dong, G. Xu, Y. Zhang, L. Shu, et al., Sevoflurane acts on ubiquitination-proteasome pathway to reduce postsynaptic density 95 protein levels in young mice, Anesthesiology 127 (6) (2017) 961–975.
[13] J. Zhang, Y. Dong, C. Zhou, Y. Zhang, Z. Xie, Anesthetic sevoflurane reduces levels of hippocalcin and postsynaptic density protein 95, Mol. Neurobiol. 51 (3) (2015) 853–863.
[14] G. Tao, J. Zhang, L. Zhang, Y. Dong, B. Yu, G. Crosby, et al., Sevoflurane induces tau phosphorylation and glycogen synthase kinase 3β activation in young mice, Anesthesiology 121 (3) (2014) 510–527.
[15] S. Gibert, N. Sabourdin, N. Louvet, M. Moutard, V. Piat, M. Guye, et al., Epileptogenic effect of sevoflurane: determination of the minimal alveolar concentration of sevoflurane associated with major epileptoid signs in children, Anesthesiology 117 (6) (2012) 1253–1261.
[16] M. Alvarado, K. Murphy, M. Baxter, Visual recognition memory is impaired in rhesus monkeys repeatedly exposed to sevoflurane in infancy, Br. J. Anaesth. 119 (3) (2017) 517–523.
[17] M. Ji, Z. Wang, X. Sun, H. Tang, H. Zhang, M. Jia, et al., Repeated neonatal sevoflurane exposure-induced developmental delays of parvalbumin interneurons and cognitive impairments are reversed by environmental enrichment, Mol. Neurobiol. 54 (5) (2017) 3759–3770.
[18] G. Xu, H. Lu, Y. Dong, D. Shapoval, S. Soriano, X. Liu, et al., Coenzyme Q10 reduces sevoflurane-induced cognitive deficiency in young mice, Br. J. Anaesth. 119 (3) (2017) 481–491.
[19] R. Epstein, E. Patai, J. Julian, H. Spiers, The cognitive map in humans: spatial navigation and beyond, Nat. Neurosci. 20 (11) (2017) 1504–1513.
[20] E. Pastalkova, P. Serrano, D. Pinkhasova, E. Wallace, A. Fenton, T. Sacktor, Storage of spatial information by the maintenance mechanism of LTP, Science (New York, NY) 313 (5790) (2006) 1141–1144.
[21] J. Tsien, P. Huerta, S. Tonegawa, The essential role of hippocampal CA1 NMDA receptor-dependent synaptic plasticity in spatial memory, Cell 87 (7) (1996) 1327–1338.
[22] R. Jackson, C. Hellen, T. Pestova, The mechanism of eukaryotic translation initiation and principles of its regulation, Nat. Rev. Mol. Cell Biol. 11 (2) (2010) 113–127.
[23] B. Schwanhäusser, D. Busse, N. Li, G. Dittmar, J. Schuchhardt, J. Wolf, et al., Global quantification of mammalian gene expression control, Nature 473 (7347) (2011) 337–342.
[24] T. Wang, Y. Cui, J. Jin, J. Guo, G. Wang, X. Yin, et al., Translating mRNAs strongly correlate to proteins in a multivariate manner and their translation ratios are phenotype specific, Nucleic Acids Res. 41 (9) (2013) 4743–4754.
[25] C. Vogel, E. Marcotte, Insights into the regulation of protein abundance from proteomic and transcriptomic analyses, Nat. Rev. Genet. 13 (4) (2012) 227–232.
[26] G. Li, D. Burkhardt, C. Gross, J. Weissman, Quantifying absolute protein synthesis rates reveals principles underlying allocation of cellular resources, Cell 157 (3) (2014) 624–635.
[27] H. Chassé, S. Boulben, V. Costache, P. Cormier, J. Morales, Analysis of translation using polysome profiling, Nucleic Acids Res. 45 (3) (2017) e15.
[28] Q. Kang, J. Pomerening, Punctuated cyclin synthesis drives early embryonic cell cycle oscillations, Mol. Biol. Cell 23 (2) (2012) 284–296.
[29] J. Chen, C. Melton, N. Suh, J. Oh, K. Horner, F. Xie, et al., Genome-wide analysis of translation reveals a critical role for deleted in azoospermia-like (Dazl) at the oocyte-to-zygote transition, Genes & development 25 (7) (2011) 755–766.
[30] I. Kronja, B. Yuan, S. Eichhorn, K. Dzeyk, J. Krijgsveld, D. Bartel, et al., Widespread changes in the posttranscriptional landscape at the Drosophila oocyte-to-embryo transition, Cell Rep. 7 (5) (2014) 1495–1508.
[31] J. Zhong, K. Magnusson, M. Swarts, C. Clendinen, N. Reynolds, S. Moffat, The application of a rodent-based Morris water maze (MWM) protocol to an investigation of age-related differences in human spatial learning, Behav. Neurosci. 131 (6) (2017) 470–482.
[32] F. Lupinacci, H. Kuasne, M. Roffé, J. Vassalakis, F. da Silva, T. Santos, et al., Polysome profiling of a human glioblastoma reveals intratumoral heterogeneity, Int. J. Mol. Sci. 20 (9) (2019).
[33] A. Bolger, M. Lohse, B. Usadel, Trimmomatic: a flexible trimmer for Illumina sequence data, Bioinformatics 30 (15) (2014) 2114–2120.
[34] A. Kechin, U. Boyarskikh, A. Kel, M. Filipenko, cutPrimers: a new tool for accurate cutting of primers from reads of targeted Next generation sequencing, J. Comput. Biol. : a journal of computational molecular cell biology 24 (11) (2017) 1138–1143.
[35] D. Kim, B. Langmead, S. Salzberg, HISAT: a fast spliced aligner with low memory requirements, Nat. Methods 12 (4) (2015) 357–360.
[36] M. Pertea, G. Pertea, C. Antonescu, T. Chang, J. Mendell, S. Salzberg, StringTie enables improved reconstruction of a transcriptome from RNA-seq reads, Nat. Biotechnol. 33 (3) (2015) 290–295.
[37] M. Robinson, D. McCarthy, G. Smyth, edgeR: a Bioconductor package for differential expression analysis of digital gene expression data, Bioinformatics 26 (1) (2010) 139–140.
[38] M. Ashburner, C. Ball, J. Blake, D. Botstein, H. Butler, J. Cherry, et al., Gene ontology: tool for the unification of biology. The Gene Ontology Consortium, Nat. Genet. 25 (1) (2000) 25–29.
[39] M. Kanehisa, M. Furumichi, M. Tanabe, Y. Sato, K. Morishima, KEGG: new perspectives on genomes, pathways, diseases and drugs, Nucleic Acids Res. 45 (2017) D353–D361.
[40] G. Yu, L. Wang, Y. Han, Q. He, clusterProfiler: an R package for comparing biological themes among gene clusters, OMICS A J. Integr. Biol. 16 (5) (2012) 284–287.
[41] A. Spandidos, X. Wang, H. Wang, B. Seed, PrimerBank: a resource of human and mouse PCR primer pairs for gene expression detection and quantification, Nucleic Acids Res. 38 (2010) D792–D799.
[42] Q. Liu, J. Trotter, J. Zhang, M. Peters, H. Cheng, J. Bao, et al., Neuronal LRP1 knockout in adult mice leads to impaired brain lipid metabolism and progressive, age-dependent synapse loss and neurodegeneration, J. Neurosci. : the official journal of the Society for Neuroscience 30 (50) (2010) 17068–17078.
[43] S. Zheng, L. An, X. Cheng, Y. Wang, Sevoflurane causes neuronal apoptosis and adaptability changes of neonatal rats, Acta Anaesthesiol. Scand. 57 (9) (2013) 1167–1174.
[44] B. Liu, Y. Gu, H. Xiao, X. Lei, W. Liang, J. Zhang, Altered metabolomic profiles may be associated with sevoflurane-induced neurotoxicity in neonatal rats, Neurochem. Res. 40 (4) (2015) 788–799.
[45] K. Kaneshwaran, M. Olah, S. Tasaki, L. Yu, E.M. Bradshaw, J.A. Schneider, et al., Sleep fragmentation, microglial aging, and cognitive impairment in adults with and without Alzheimer's dementia, Sci. Adv. 5 (12) (2019) eaax7331.
[46] L.M. Brito, A. Ribeiro-Dos-Santos, A.F. Vidal, G.S. de Araujo, Differential expression and miRNA-gene interactions in early and late mild cognitive impairment, Biology 9 (9) (2020).
[47] L. Kaczmarczyk, M. Schleif, L. Dittrich, R.H. Williams, M. Koderman, V. Bansal, et al., Distinct translatome changes in specific neural populations precede electroencephalographic changes in prion-infected mice, PLoS Pathog. 18 (8) (2022) e1010747.